ISR perp. to $\mathbf{B}$

Erhan Kudeki — ECE, UIUC

June 2006

Incoherent-scatter spectral models for modes propagating perpendicular to Earth's magnetic field $\mathbf{B}$ will be described.

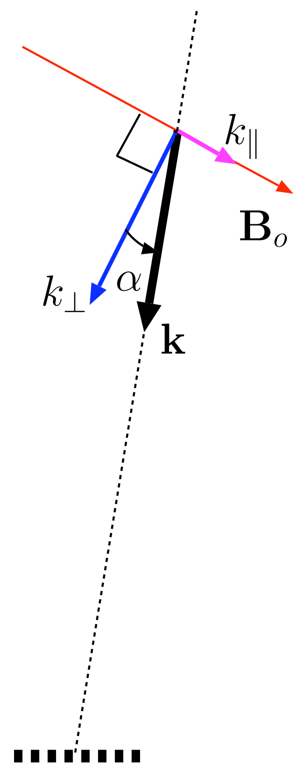

Outline:

- **Motivation:** Why "perp. to $\mathbf{B}$ ISR" is important?
- **ISR tutorial:** to establish a setting needed for the discussion of perp. to $\mathbf{B}$ issues.
- Recent results on the effect of electron Coulomb collisions (1996-2004).
- 3-D modeling of collision effects — also in *Milla and Kudeki* [2006] poster.

Why "perp. to $\mathbf{B}$ ISR theory" is important?

Because:

- "Perp. to $\mathbf{B}$" is the **natural look direction** for equatorial ISR (JRO, ALTAIR, AMISR(?)) *vertical drift measurements*.
- **ISR spectrum** is *very different* at small aspect angles α, close to perp to $\mathbf{B}$ — familiar **double-humped** shape disappears as "overspread" scatter turns into "underspread" in $\alpha \rightarrow 0$ limit.
- Different spectral shapes correspond to different micro-physics dominant at different aspect angles.
- ISR theory had to be revised a number of times (over the last 40 years) in small-α regime to match the increasingly refined new observations coming from JRO — we are currently going through another round of revisions.
- Revisions are related to difficult issues in plasma physics concerning collisions and thus the results could have **"broader impact"**.

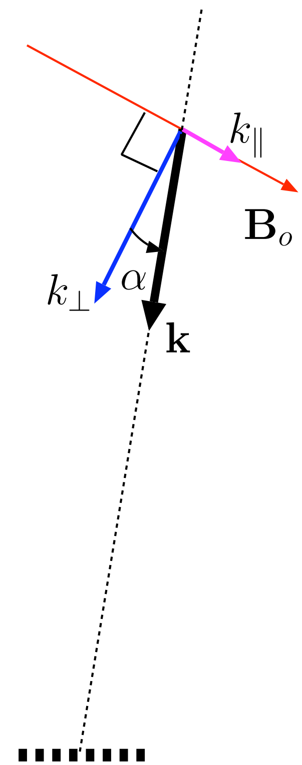

- ISR spectrum narrows down to "almost a *delta*" as $\alpha \to 0$, which is wonderful for high-precision drift measurements using "periodogram" techniques.
- A better understanding of the ISR spectrum for small-α opens up the possibility of density and temperature measurements that accompany drift observations — **practical impact**.
- Perp. to $\mathbf{B}$ direction is also the natural direction to observe *field-aligned plasma instabilities* — e.g., spread-F, 150-km echoes, electrojet in the equatorial ionosphere.
- Joint studies of the instabilities and surrounding ionosphere can be conducted by using perp. to $\mathbf{B}$ radar beams — another **practical reason**.

Now the tutorial ...

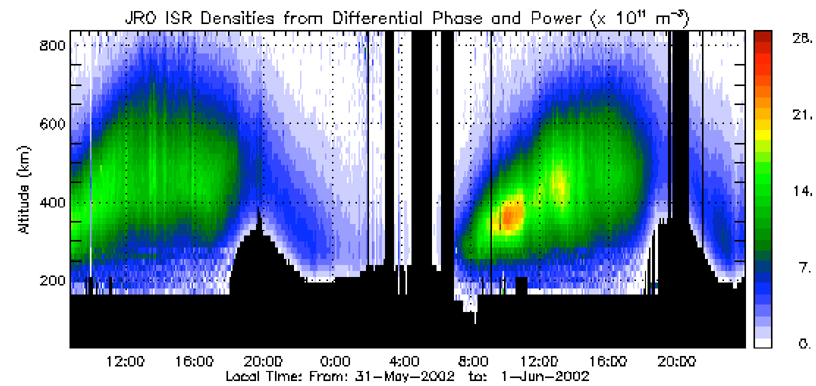

using differential phase method [*Feng et al.*, 2004]

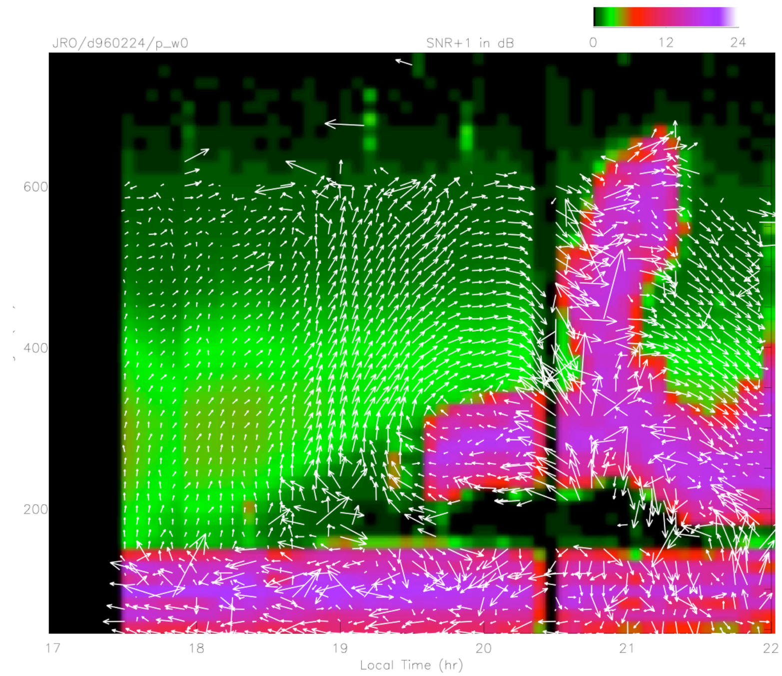

such observations have lead to significant progress in explaining bottom-type spread-F [*Kudeki and Bhattacharyya*, 1999] and shear-driven seeding of spread-F bubbles [*Hysell and Kudeki*, 2004]

First degree of α:

From *Milla and Kudeki* poster [2006] showing the results of *brand new* collisional ISR spectrum calculations using a 3-D random walk code — just in case I get stuck in the tutorial and run out of time:

$\text{Re}\{J_e(\omega)\}$ at 50 MHz:

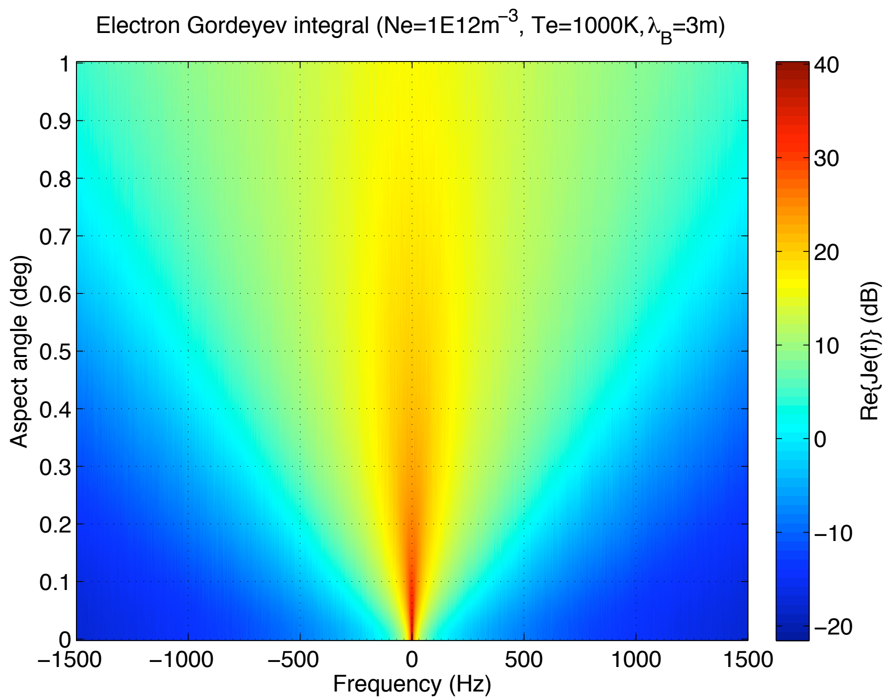

$\text{Re}\{J_e(\omega)\}$ at 500 MHz:

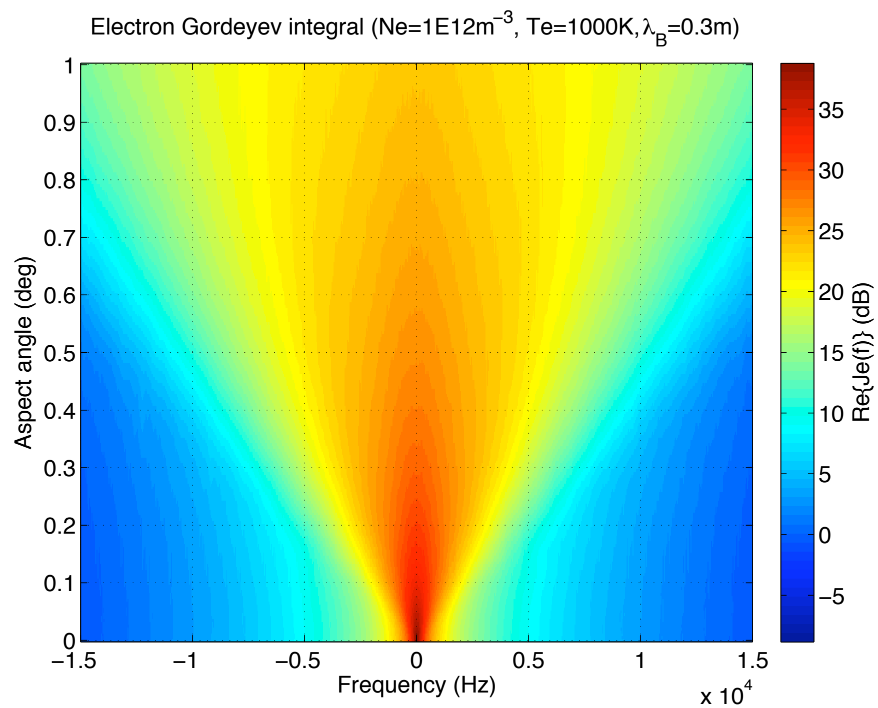

Unless electron Coulomb collisions are included in the theory, the narrowing of the spectrum in $\alpha \to 0$ limit is not properly modeled. — **Now the tutorial, really ...**

for 0.25 to 0 deg aspect angles the results are totally new at 50 MHz...

Thomson scatter from a single electron

Oscillating free electrons radiate like Hertzian dipoles:

$$E_s e^{j\omega_o t} = -\frac{r_e}{r} E_i e^{j(\omega_o t - 2k_o r)}$$

is the electric field "backscattered" or "radiated back" from a single electron at a distance r in response to an incident field (real parts are implied in both expressions)

$$E_i e^{j(\omega_o t - k_o r)}$$

of frequency ω_o and wavenumber $k_o = \frac{\omega_o}{c} = \frac{2\pi}{\lambda_o}$;

$$r_e \equiv \frac{e^2}{4\pi\epsilon_o mc^2} \approx 2.818 \times 10^{-15}\,\mathrm{m}$$

is a fundamental length scale known as *classical electron radius*.

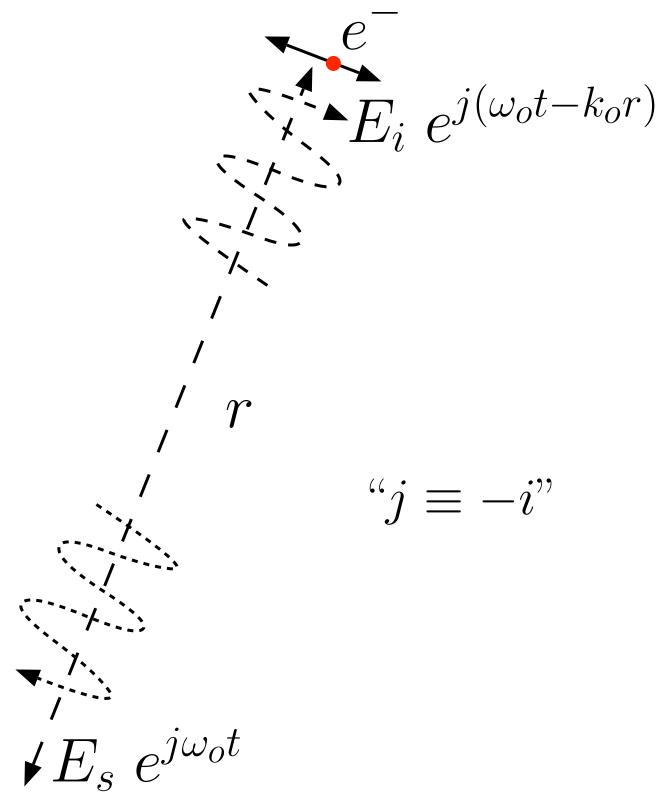

"$j \equiv -i$"

Backscatter from a small volume of electrons

Backscattered field envelope from a small volume ΔV centered at $\mathbf{r} = r\hat{r}$ containing P free electrons at an average-density of $N_o = P/\Delta V$ is the simple sum

$$E_s \quad = \quad -\sum_{p=1}^{N_o \Delta V} \frac{r_e}{r_p} E_{ip}\, e^{-j2k_o r_p} \rightarrow -\frac{r_e}{r} E_i \sum_{p=1}^{N_o \Delta V} e^{j\mathbf{k}\cdot\mathbf{r_p}}.$$

The paraxial limit on the right is valid for $r > 4\Delta V^{2/3}/\lambda_o$ (effectively the far-field condition for an antenna of size $\Delta V^{1/3}$ and wavelength $\lambda_o/2$) while

$$\mathbf{k} \equiv -2k_o\hat{r},$$

known as *Bragg vector*, is the scattered minus incident wavevector relevant to scattering volume ΔV.

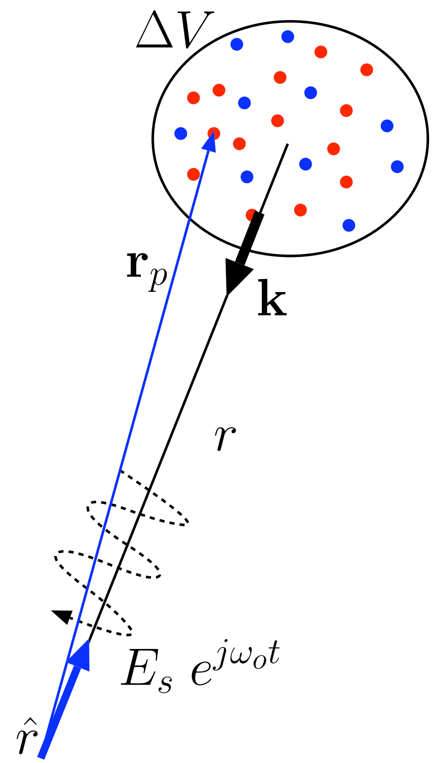

Particle trajectories $\mathbf{r}_p(t)$ and density-waves $n(\mathbf{k},t)$:

The scattered field varies with time as

$$E_s(t) = -\frac{r_e}{r} E_i \sum_{p=1}^{N_o \Delta V} e^{j\mathbf{k}\cdot\mathbf{r_p}(t)} = -\frac{r_e}{r} E_i \, n(\mathbf{k},t)$$

where

$$n(\mathbf{k},t) \equiv \sum_{p=1}^{N_o \Delta V} e^{j\mathbf{k}\cdot\mathbf{r_p}(t)}$$

is the *spatial* Fourier transform $\int d\mathbf{r}\, n(\mathbf{r},t)\, e^{j\mathbf{k}\cdot\mathbf{r}}$ of

$$n(\mathbf{r},t) = \sum_{p=1}^{N_o \Delta V} \delta(\mathbf{r} - \mathbf{r}_p(t)),$$

a *number density function* defined for electrons with trajectories $\mathbf{r}_p(t)$.

Note: Normalized *variance*

$$\frac{1}{\Delta V}\langle |n(\mathbf{k},t)|^2 \rangle$$

in $\Delta V \rightarrow \infty$ limit (meaning $\Delta V^{1/3} >$ a few *correlation scales*) is the *spatial* power spectrum of density fluctuations due to random trajectories $\mathbf{r}_p(t)$.

Density *space-time* spectrum is (likewise) the Fourier transform of normalized auto-correlation (ACF)

$$\frac{1}{\Delta V}\langle n^*(\mathbf{k},t) n(\mathbf{k},t+\tau) \rangle$$

of $n(\mathbf{k},t)$ over time lag τ (see next page).

"Soft-target" power spectra

$$E_s(t) = -\frac{r_e}{r} E_i\, n(\mathbf{k}, t) \quad \Rightarrow \quad \langle |E_s(\omega)|^2 \rangle = \frac{r_e^2}{r^2} |E_i|^2 \langle |n(\mathbf{k}, \omega)|^2 \rangle \Delta V$$

in terms of electron-density space-time spectrum

$$\langle |n(\mathbf{k}, \omega)|^2 \rangle \quad \equiv \quad \int d\tau e^{-j\omega\tau} \frac{1}{\Delta V} \langle \sum_{p=1}^{N_o \Delta V} e^{-j\mathbf{k}\cdot\mathbf{r}_\mathbf{p}(t)} \sum_{p=1}^{N_o \Delta V} e^{j\mathbf{k}\cdot\mathbf{r}_\mathbf{p}(t+\tau)} \rangle$$

Also the *total power* collected by a radar antenna with an effective aperture A_e — adding the spectrum over all frequencies $\omega/2\pi$ and subvolumes ΔV — is (open-bandwidth case)

$$P_r = \int \frac{d\omega}{2\pi} \int dV \; \frac{|E_i|^2/2\eta_o}{r^2} A_e r_e^2 \langle |n(\mathbf{k}, \omega)|^2 \rangle \quad \text{—\textit{Radar eqn.}}$$

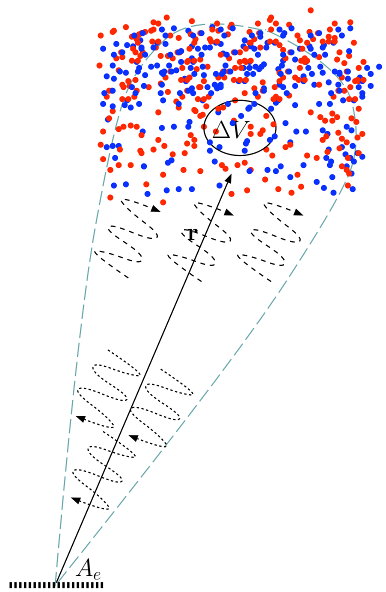

$\langle |n(\mathbf{k}, \omega)|^2 \rangle$ is the F.T. over time lag τ of the normalized ACF

$$\frac{1}{\Delta V} \langle n^*(\mathbf{k}, t) n(\mathbf{k}, t + \tau) \rangle.$$

Above and elsewhere, angular brackets ⟨ and ⟩ around a random variable imply an *expected value* or *ensemble average*.

"Soft-target" power spectra

$$E_s(t) = -\frac{r_e}{r} E_i\, n(\mathbf{k}, t) \quad \Rightarrow \quad \langle |E_s(\omega)|^2 \rangle = \frac{r_e^2}{r^2} |E_i|^2 \langle |n(\mathbf{k}, \omega)|^2 \rangle \Delta V$$

in terms of electron-density space-time spectrum

$$\langle |n(\mathbf{k}, \omega)|^2 \rangle = \int d\tau e^{-j\omega\tau} \frac{1}{\Delta V} \langle \sum_{p=1}^{N_o \Delta V} e^{-j\mathbf{k}\cdot\mathbf{r_p}(t)} \sum_{p=1}^{N_o \Delta V} e^{j\mathbf{k}\cdot\mathbf{r_p}(t+\tau)} \rangle$$

$$= N_o \int d\tau e^{-j\omega\tau} \langle e^{j\mathbf{k}\cdot\Delta\mathbf{r}} \rangle \equiv \langle |n_{te}(\mathbf{k}, \omega)|^2 \rangle,$$

assuming that electrons follow random trajectories with independent displacements $\Delta\mathbf{r} \equiv \mathbf{r}(t+\tau) - \mathbf{r}(t)$. But the assumption is not valid, and its direct consequence (in thermal equilibrium)

$$\langle |E_s(\omega)|^2 \rangle \propto \langle |n_{te}(\mathbf{k}, \omega)|^2 \rangle \propto \int d\tau e^{-j\omega\tau} \langle e^{j\mathbf{k}\cdot\mathbf{v}\tau} \rangle \propto e^{-\frac{\omega^2}{2k^2 C_e^2}},$$

a Gaussian radar spectrum of a width $\propto$ electron thermal speed C_e — original expectation of *Gordon* [1958] — is not observed.

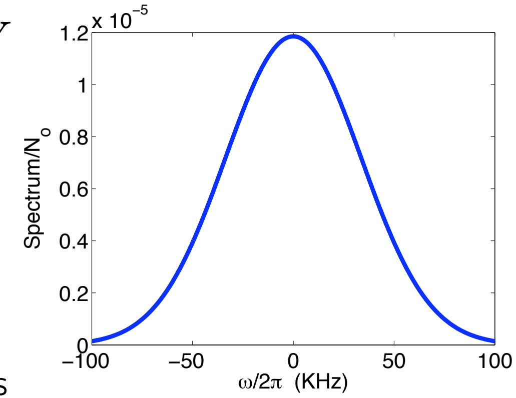

Not this

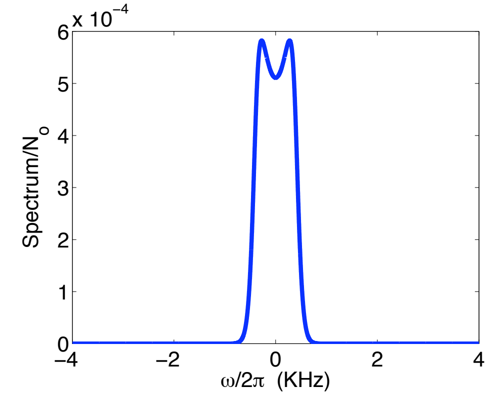

but this

because of "collective effects" due to polarization fields (spectra for 41 MHz observations of *Bowles*, 1958).

Including the "collective effects"

If there were no collective effects

- spectrum of electron and ion density fluctuations in the plasma would be

$$\langle |n_{te,i}(\mathbf{k},\omega)|^2 \rangle \equiv N_o \int_{-\infty}^{\infty} d\tau e^{-j\omega\tau} \langle e^{j\mathbf{k}\cdot\Delta\mathbf{r}_{e,i}} \rangle ,$$

  with

  - N_o average plasma density
  - $\Delta\mathbf{r}_{e,i} \equiv \mathbf{r}_{e,i}(t+\tau) - \mathbf{r}_{e,i}(t)$ independent particle displacements

- of course there would also be random *current densities* "$\frac{\omega}{k} e(n_{ti} - n_{te})$" and *space-charge* fluctuations "$e(n_{ti} - n_{te})$" satisfying the plane-wave *continuity equation* across $\mathbf{k}$-ω space

Collective effects come into play because space-charge $\propto n_{ti} - n_{te}$ requires (via Poisson's equation) a longitudinal electric field E (parallel to $\mathbf{k}$) which, in turn, drives additional currents $\sigma_e E$ and $\sigma_i E$ to *force* the *total current*, including the displacement current $j\omega\epsilon_o E$, to vanish; thus

$$(j\omega\epsilon_o + \sigma_e + \sigma_i)E + \frac{\omega}{k}e(n_{ti} - n_{te}) = 0$$

so that Ampere's law applied to longitudinal (space-charge) waves (influenced by collective effects) is satisfied.

One of the solutions of this "KCL equation" — obtained with the aid of an equivalent circuit model shown below — is the electron-density wave amplitude

$$n(\mathbf{k},\omega) = \frac{(j\omega\epsilon_o + \sigma_i)n_{te}(\mathbf{k},\omega)}{j\omega\epsilon_o + \sigma_e + \sigma_i} + \frac{\sigma_e n_{ti}(\mathbf{k},\omega)}{j\omega\epsilon_o + \sigma_e + \sigma_i},$$

a weighted sum that can be interpreted in terms of "shielded" versions of thermally driven densities n_{te} and n_{ti} — shielding reduces the overall space-charge by a factor $|1 + \chi_e + \chi_i| \gg 1$, where $\chi_{e,i} \equiv \sigma_{e,i}/j\omega\epsilon_o$ are electron- and ion-susceptibilities.

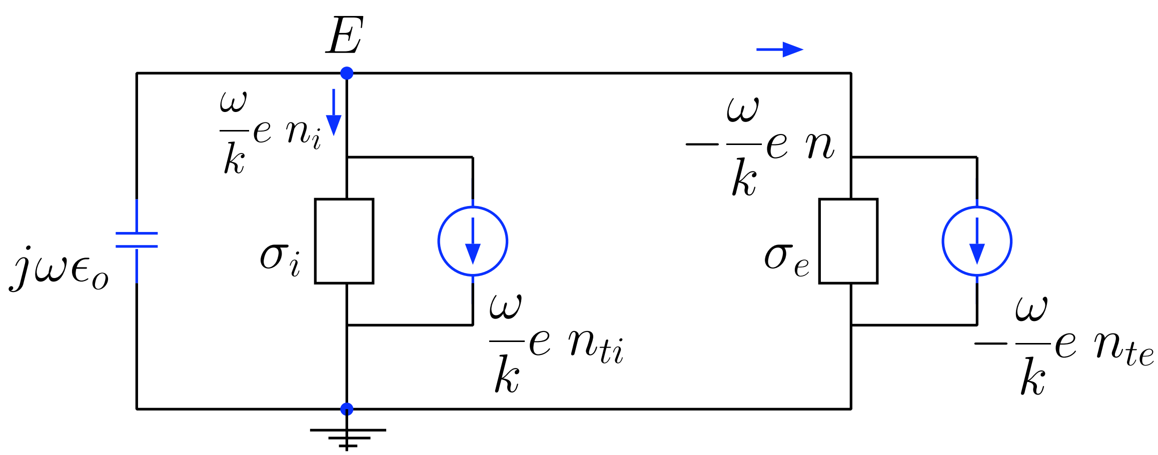

We have expressed the actual electron density fluctuation in the plasma in terms of independent random variables n_{te} and n_{ti}; thus, upon squaring and averaging the expression we find that electron density spectrum

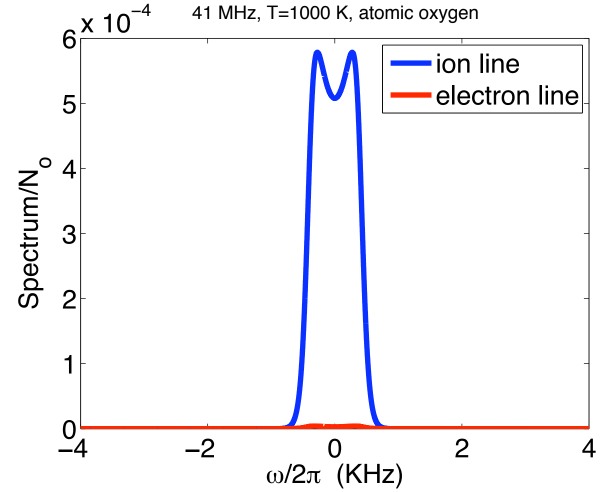

$$\langle|n(\mathbf{k},\omega)|^2\rangle = \frac{|j\omega\epsilon_o+\sigma_i|^2\langle|n_{te}(\mathbf{k},\omega)|^2\rangle}{|j\omega\epsilon_o+\sigma_e+\sigma_i|^2} + \frac{|\sigma_e|^2\langle|n_{ti}(\mathbf{k},\omega)|^2\rangle}{|j\omega\epsilon_o+\sigma_e+\sigma_i|^2},$$

a sum of electron- and ion-*lines*, proportional to $\langle|n_{te,i}(\mathbf{k},\omega)|^2\rangle$, respectively.

The spectrum formula above is a very general result which is valid with any type of velocity distribution (i.e., Maxwellian or not). It can be modified in a straightforward way to treat the multi-ion case. It is also valid in magnetized plasmas in electrostatic approximation — i.e., for nearly longitudinal modes with phase speeds $\omega/k \ll c$ — with $\sigma_{e,i} = \sigma_{e,i}(\mathbf{k},\omega)$ denoting the longitudinal component of particle conductivities. However, to use it we need accurate knowledge of all $\sigma_{e,i}(\mathbf{k},\omega)$.

Fortunately, there are some wonderful *links* between conductivities $\sigma_{e,i}(\mathbf{k},\omega)$ and $e^{j\mathbf{k}\cdot\Delta\mathbf{r}}$-statistics of particles that we can use.

Links

First, according to generalized *Nyquist noise* theorem [e.g., *Callen and Greene*, 1952], *mean-squared particle current* due to random thermal motions is (in the particle frame)

$$\frac{\omega^2}{k^2} e^2 \langle |n_{te,i}(\mathbf{k},\omega)|^2 \rangle = 2KT_{e,i} \mathrm{Re}\{\boldsymbol{\sigma}_{e,i}(\mathbf{k},\omega)\}$$

per unit bandwidth, per species, so long as each species is in thermal equilibrium (i.e., have a Maxwellian velocity distribution) at a temperature[1] $T_{e,i}$.

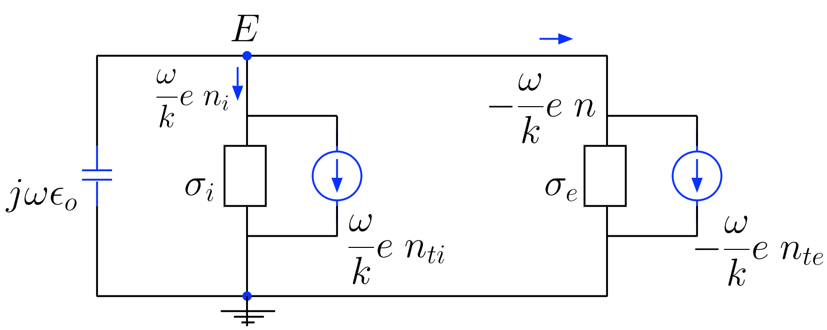

[1] When $T_e = T_i = T$, i.e., in case of full thermal equilibrium, $\frac{\omega^2}{k^2} e^2 \langle |n(\mathbf{k},\omega)|^2 \rangle = 2KT\mathrm{Re}\{\sigma_t(\mathbf{k},\omega)\}$ with σ_t representing the Thevenin admittance of the equivalent circuit looking into the opened electron branch.

Second, as a consequence of *causality*, imaginary part $\mathrm{Im}\{\sigma_{e,i}(\mathbf{k},\omega)\}$ of conductivity $\sigma_{e,i}(\mathbf{k},\omega)$ is the *Hilbert transform* of $\mathrm{Re}\{\sigma_{e,i}(\mathbf{k},\omega)\}$, a general rule known as *Kramers-Kronig relation* which applies to all Fourier transforms of causal signals that vanish for $t < 0$.

The upshot is, in a plasma in thermal equilibrium, all parameters needed to compute the electron density spectrum can be deduced from

$$\langle e^{j\mathbf{k}\cdot\Delta\mathbf{r}_{e,i}}\rangle,$$

characteristic functions of particle displacements $\Delta\mathbf{r}_{e,i}$ in the absence of collective effects. We will call them "single particle ACF's" in the following discussions.

What we have seen so far was *distilled* from a number of different approaches to incoherent scatter problem worked out during the 1960's:

- *Farley* and co-writers derive $\sigma_{e,i}(\mathbf{k},\omega)$ from plasma kinetic theory (Vlasov equation) and then use the Nyquist formula to obtain $\langle |n_{te,i}(\mathbf{k},\omega)|^2\rangle$.
- *Fejer* does both calculations independently, not using (but effectively re-deriving) the Nyquist formula.
- *Woodman* takes yet another approach, including steps involved in the proof of the generalization of Nyquist theorem by *Callen and Greene* [1952], but not using Nyquist's formula explicitly.
- *Hagfors* and collaborators first calculate $\langle |n_{te,i}(\mathbf{k},\omega)|^2\rangle$ from $\langle e^{j\mathbf{k}\cdot\Delta\mathbf{r}_{e,i}}\rangle$ and then "dress" the particles making up $n_{te,i}(\mathbf{k},\omega)$ with $\sigma_{e,i}(\mathbf{k},\omega)$ dependent "shields" to obtain the expression for electron density spectrum — Nyquist formula is effectively re-derived.

These pioneers have handed us (the current generation of ISR users) a ...

“Standard Model”

$$J_s(\omega) \equiv \int_0^\infty d\tau\, e^{-j\omega\tau} \langle e^{j\mathbf{k}\cdot\Delta\mathbf{r}_s} \rangle$$ — *Gordeyev integral, a 1-sided F.T.*

for species s (e or i for the single-ion case), and use

$$\frac{\langle |n_{ts}(\mathbf{k},\omega)|^2 \rangle}{N_o} = 2\mathrm{Re}\{J_s(\omega_s)\} \quad \text{and} \quad \frac{\sigma_s(\mathbf{k},\omega)}{j\omega\epsilon_o} = \frac{1 - j\omega_s J_s(\omega_s)}{k^2 h_s^2},$$

where $\omega_s \equiv \omega - \mathbf{k}\cdot\mathbf{V}_s$ is Doppler-shifted frequency in the radar frame due to mean velocity $\mathbf{V}_s$ of the species and $h_s = \sqrt{\epsilon_o K T_s / N_o e^2}$ is the corresponding Debye length. In terms of above definitions, electron density spectrum of a stable Maxwellian plasma is

$$\langle |n(\mathbf{k},\omega)|^2 \rangle = \frac{|j\omega\epsilon_o + \sigma_i|^2 \langle |n_{te}(\mathbf{k},\omega)|^2 \rangle}{|j\omega\epsilon_o + \sigma_e + \sigma_i|^2} + \frac{|\sigma_e|^2 \langle |n_{ti}(\mathbf{k},\omega)|^2 \rangle}{|j\omega\epsilon_o + \sigma_e + \sigma_i|^2}.$$

The model takes care of *macro*physics of incoherent scatter — *micro*physics details need to be addressed within single particle ACF's $\langle e^{j\mathbf{k}\cdot\Delta\mathbf{r}_s} \rangle$.

Single particle ACFs $\langle e^{j\mathbf{k}\cdot\Delta\mathbf{r}}\rangle \equiv \langle e^{j\mathbf{k}\cdot(\mathbf{r}(t+\tau)-\mathbf{r}(t))}\rangle$

are the *centerpiece* of Standard Model — their Fourier transforms or *Gordeyev integrals* (obtained numerically in most cases) provide us with the conductivities and spectra of all species in a plasma (in thermal equilibrium).

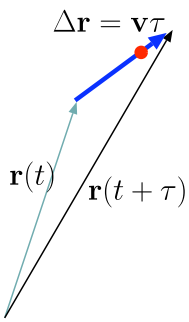

In general, if Δr, component of $\Delta\mathbf{r}$ along $\mathbf{k}$, is a Gaussian random variable, then

$$\langle e^{j\mathbf{k}\cdot\Delta\mathbf{r}}\rangle = e^{-\frac{1}{2}k^2\langle\Delta r^2\rangle}.$$

Example: In a *non-magnetized plasma* particles move along *straight line trajectories* (in between collisions) with velocities $\mathbf{v}$ and thus

$$\Delta\mathbf{r} = \mathbf{v}\tau;$$

hence

$$\Delta r = v\tau \quad \Rightarrow \quad \langle\Delta r^2\rangle = \langle v^2\rangle\tau^2 = C^2\tau^2,$$

for a Maxwellian (required by Standard Model) distributed v along $\mathbf{k}$ with an rms speed $\langle v^2\rangle^{1/2} = \sqrt{KT/m} \equiv C$. Thus, in a non-magnetized plasma

$$\langle e^{j\mathbf{k}\cdot\Delta\mathbf{r}}\rangle = e^{-\frac{1}{2}k^2C^2\tau^2}$$

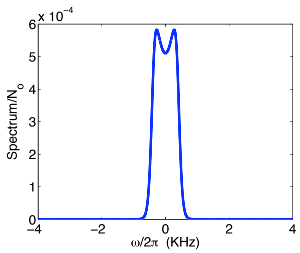

and "Ohmic" σ's because of Landau damping (inherent to Std. Model).

so long as "collision frequency" ν is small compared to kC — i.e., if an average particle moves a distance of many wavelengths $\frac{2\pi}{k}$ in between collisions.

In a collisional plasma $\langle \Delta r^2 \rangle = C^2\tau^2$, special for free-streaming particles, stays valid until "first collisions" take place at $\tau \sim \nu^{-1}$. For $\nu\tau \gg 1$, collisional random walk process leads to $\langle \Delta r^2 \rangle \propto \tau$ instead of τ^2, and more specifically, over all τ,

Collisional D-region spectra from JRO:

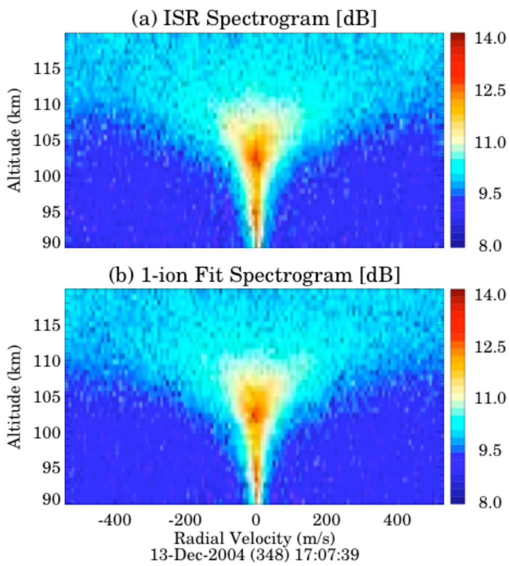

Chau and Kudeki [2006]

$$\langle \Delta r^2 \rangle = \frac{2C^2}{\nu^2}(\nu\tau - 1 + e^{-\nu\tau}) \;\Rightarrow\; \mathrm{ACF} = \begin{cases} e^{-\frac{1}{2}k^2C^2\tau^2}, & \nu \ll kC \\ e^{-\frac{k^2C^2}{\nu}\tau}, & \nu \gg kC \end{cases}$$

if a *Brownian-motion model* is adopted for collisions. Using the high-collision approximation above (which is not sensitive to the choice collision model, e.g., Brownian, BGK, etc.) a *Lorentzian shaped* electron density spectrum pertinent to D-region altitudes can be easily obtained (mainly the "ion-line"):

$$\frac{\langle |n(\mathbf{k},\omega)|^2 \rangle}{N_o} \approx \frac{2k^2D_i}{\omega^2 + (2k^2D_i)^2}$$

in $kh \ll 1$ limit (wavelength larger than Debye length) with $D_i \equiv C_i^2/\nu_i = KT_i/m_i\nu_i$, ion diffusion coefficient.

However, a complete D-region model should require a multi-ion formulation including negative ions [e.g., *Mathews*, 1978].

Generalizations:

Using the above result, it is easy to show that

$$\langle |n(\mathbf{k})|^2 \rangle \equiv \int_{-\infty}^{\infty} \frac{d\omega}{2\pi} \langle |n(\mathbf{k},\omega)|^2 \rangle = \frac{N_o}{2},$$

which is in fact true *in general* — i.e., for all types of plasmas with or without collisions and/or DC magnetic field — so long as $T_e = T_i$ and $kh \ll 1$.

This result in turn leads to a well-known volumetric radar cross-section formula for incoherent backscatter (valid under the same conditions):

$$4\pi r_e^2 \langle |n(\mathbf{k})|^2 \rangle = 2\pi r_e^2 N_o.$$

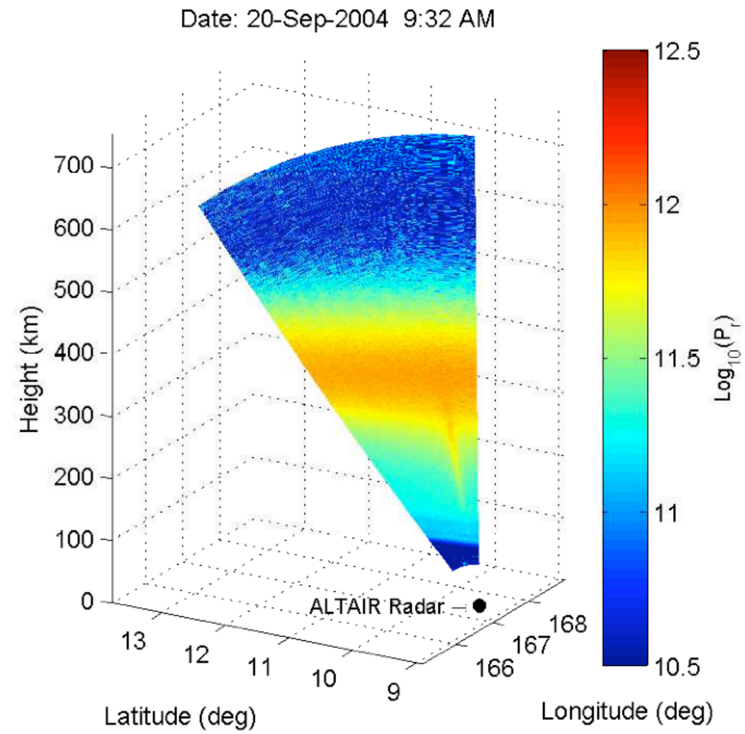

Notice *aspect angle* dependent errors from 200 to 300 km where $T_e > T_i$.

Only for $kh \gg 1$ we obtain $\langle |n(\mathbf{k})|^2 \rangle = N_o$.

Plasma with a DC magnetic $\mathbf{B}_o$

$$\langle e^{j\mathbf{k}\cdot\Delta\mathbf{r}}\rangle = \langle e^{j(k_\parallel \Delta r + k_\perp \Delta p)}\rangle = \langle e^{jk_\parallel \Delta r} \times e^{jk_\perp \Delta p}\rangle,$$

where Δr and Δp are particle displacements along and perp to $\mathbf{B}_o$ on $\mathbf{k}$-$\mathbf{B}_o$ plane.

Assuming independent Gaussian random variables Δr and Δp, we can write

$$\langle e^{j\mathbf{k}\cdot\Delta\mathbf{r}}\rangle = e^{-\frac{1}{2}k_\parallel^2\langle\Delta r^2\rangle} \times e^{-\frac{1}{2}k_\perp^2\langle\Delta p^2\rangle}$$

in analogy with non-magnetized case. The assumptions are valid in the absence of collisions, in which case

$$\langle\Delta r^2\rangle = C^2\tau^2 \quad \textit{and} \quad \langle\Delta p^2\rangle = \frac{4C^2}{\Omega^2}\sin^2(\Omega\tau/2),$$

where Ω is the gyro-frequency and periodic $\langle\Delta p^2\rangle$ is fairly easy to confirm in terms of circular orbits with periods $2\pi/\Omega$ and mean radii $\sqrt{2}C/\Omega$.

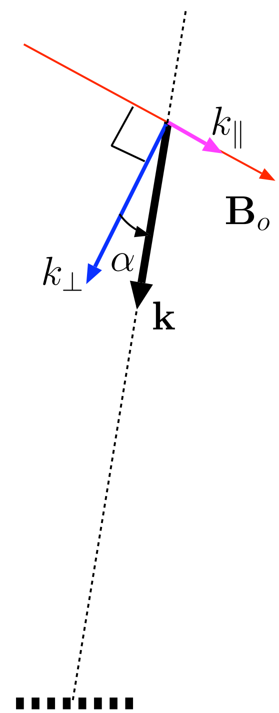

Thus,

$$\langle e^{j\mathbf{k}\cdot\Delta\mathbf{r}}\rangle = e^{-\frac{1}{2}k_{\parallel}^2 C^2 \tau^2} \times e^{-\frac{2k_{\perp}^2 C^2}{\Omega^2}\sin^2(\Omega\tau/2)}$$

Spectrum examples:

Large α : the usual ion-line

Small α: "electron-line" with a reduced width

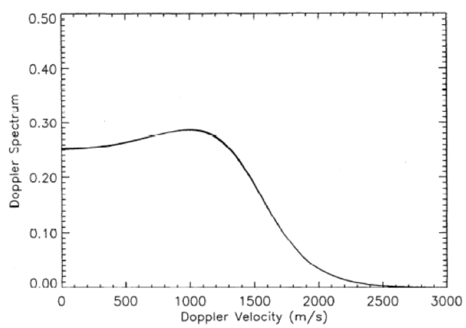

Figure 1. Incoherent scatter Doppler spectra for $\alpha = 30^o, 60^o, 90^o$ are shown in a superposed form. The curves represent an O^+ plasma with $T_e = T_i = 1000$ K and a radar carrier frequency of 50 MHz and are essentially indistinguishable at the scale of the plot.

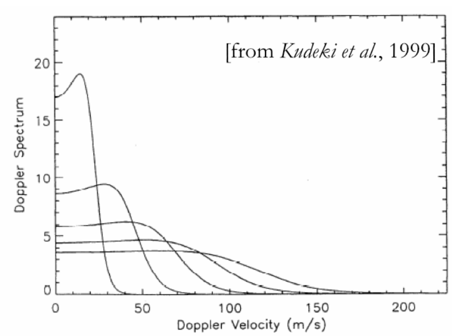

Figure 2. Same as Figure 1, but for $\alpha = 0.005^o, 0.01^o, 0.015^o, 0.02^o$. The tallest curve corresponds to $\alpha = 0.005^o$ and the broadest curve to $\alpha = 0.02^o$.

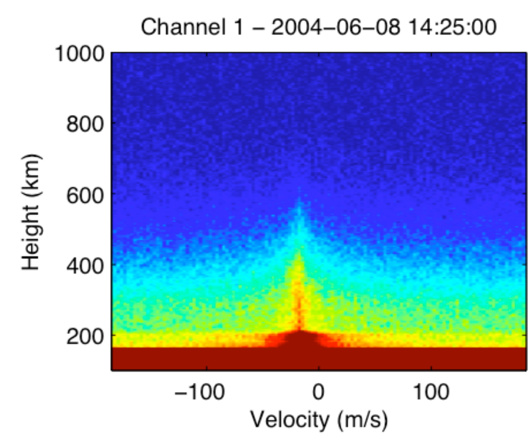

Note, the ACF above becomes periodic and the associated spectra are singular (with delta functions) in $k_{\parallel} \rightarrow 0$ limit. Singularities are not observed in practice and it was recognized early on to include *Coulomb collisions* — electrostatic interactions of neraby particles within a Debye length not covered by collective effects — in the theory [*Farley,* 1964]. Examples above were obtained with collisional equations of *Woodman* [1967] that includes ion-ion collisions.

After Sept 94 MISETA experiments we started applying the same spectral analysis to SpF and ISR data...
****
The new method provided much better precision and resolution than the ACF methods used in the past...******
But, our efforts to fit Te gave unrealistically low results, at least by a factor of 2

And then there was the puzzle of Te<Ti being estimated at 2 deg off-perp --- since the 60's, in fact --- with major efforts put by Pingree [1990] to understand the reason

A collisional/magnetized model, consistent with independent and Gaussian Δr and Δp assumptions, is obtained with

$$\langle \Delta r^2 \rangle = \frac{2C^2}{\nu^2}(\nu\tau - 1 + e^{-\nu\tau}),$$
$$\langle \Delta p^2 \rangle = \frac{2C^2}{\nu^2+\Omega^2}(\cos(2\gamma) + \nu\tau - e^{-\nu\tau}\cos(\Omega\tau - 2\gamma)),$$

where $\gamma \equiv \tan^{-1}\nu/\Omega$ — first derived by *Woodman* [1967] using what is effectively a Brownian motion model in the presence of $\mathbf{B}_o$. In perp to $\mathbf{B}_o$ limit:

$$\langle e^{j\mathbf{k}\cdot\Delta\mathbf{r}} \rangle \rightarrow e^{-\frac{k^2C^2}{\Omega^2+\nu^2}(\cos(2\gamma)+\nu\tau-e^{-\nu\tau}\cos(\Omega\tau-2\gamma))}$$

is non-periodic, ion resonances go-away, electron-line is broadened:

Effective (velocity averaged) Coulomb collision frequencies for a singly ionized plasma (after *Spitzer*, 1958):

$$\nu_e = \frac{4\sqrt{2\pi}N_i e^4 \ln(12\pi N_e h_e^3)}{3(4\pi\epsilon_o)^2\sqrt{m_e T_e^3}} \propto \frac{N_i}{T_e^{3/2}},$$

$$\nu(v) = \frac{4\pi N_i e^4 \ln\Lambda}{(4\pi\epsilon_o)^2 m_e^2 v^3}, \nu_i = \sqrt{\frac{m_e T_e^3}{2m_i T_i^3}}\nu_e$$

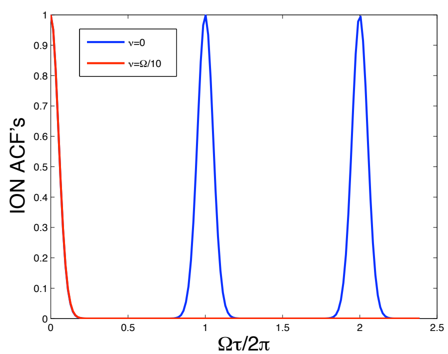

Ion-line gyro-resonances are suppressed.

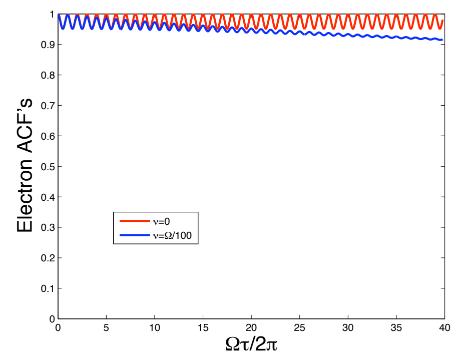

electron-line is broadened to $\nu_e k^2 C_e^2/\Omega_e^2$

... but what we wanted at that point was spectral narrowing, not broadening !!!

While electron collisions cause spectral broadening at $\alpha = 0$ (by enabling cross-field diffusion), their effect turns out to be in the opposite direction at small but non-zero α because of parallel-dynamics:

$$e^{-\frac{k_{\|}^2 C^2}{\nu^2}(\nu\tau - 1 + e^{-\nu\tau})} \rightarrow \begin{cases} \sim e^{-\frac{1}{2}k_{\|}^2 C^2 \tau^2}, \; \nu \ll k_{\|}C & \text{— free streaming} \\ \sim e^{-\frac{k_{\|}^2 C^2}{\nu}\tau}, \quad \nu \gg k_{\|}C & \text{— diffusion limit} \end{cases}$$

- first line above, valid at larger α or $k_{\|}$, accounts for the usual narrowing of electron-line with decreasing α in the absence of collisions,
- the second line, valid for smaller α, predicts additional narrowing due to collisions, just like in D-region narrowing of ion-line with increasing ν — basically, collisions impede motion along $\mathbf{B_o}$, lengthening correlation times and narrowing the corresponding spectra. However, the narrowing effect is still quite weak at $\alpha \approx 2^{\circ}$ when the Brownian collision model is used.

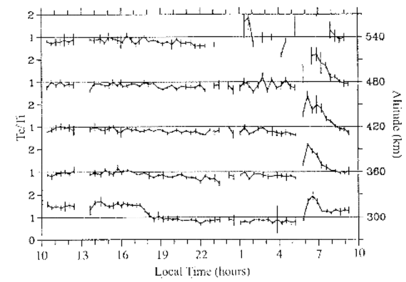

Figure 3. Jicamarca T_e/T_i for selected heights on June 16-17, 1988, using the 3° antenna position (adapted from *Pingree* [1990]).

from *Aponte et al.* [2001], illustrating $T_e/T_i < 1$.

Sulzer and Gonzalez [1999] conjectured that a proper treatment of electron Coulomb collisions should do the job — i.e., eliminate non-physical results of $T_e < T_i$ inferred from JRO F-region data taken at $\alpha \approx 2^{\circ}$ [e.g., *Pingree*, 1990] — and proved their point by simulating the Coulomb collision process for electrons.

Sulzer and Gonzalez [1999] & Woodman [2004]:

The Brownian motion model is based on an assumption of constant collision/diffusion coefficients in a governing "Langevin equation" — a 1st order stochasic differential equation governing electron velocity $v(t)$ [e.g., *Gillespie*, 1996] — whereas, "in reality", the coefficients for Coulomb collisions are $v(t)$ dependent. Thus in reality the equation for $v(t)$ is non-linear, causing the statistics of $v(t)$ and its time integral Δr to become non-Gaussian. To address this difficulty and explore its implications, *Sulzer and Gonzalez* [1999] computed the electron ACF $\langle e^{j\mathbf{k}\cdot\Delta\mathbf{r}}\rangle$ numerically using a Monte Carlo approach:

The positions and velocities $\mathbf{r}(t)$ and $\mathbf{v}(t)$ of simulated electron motions were updated at Δt intervals with increments

$$\Delta\mathbf{r} = \mathbf{v}\Delta t$$

and

$$\Delta\mathbf{v} = \mathbf{K}\Delta t + \delta\mathbf{v},$$

where $\delta\mathbf{v}$ is a Gaussian random variable with $\mathbf{v}$ and Δt dependent moments — derived specifically for Coulomb collisions by *Rosenbluth et al.* [1957] and others dating back to *Chandrasekhar* [1942] — and $\mathbf{K}$ is a deterministic external force per unit mass.

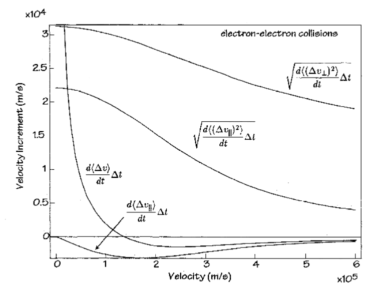

Figure 2. Functions derived from the diffusion coefficients for electron-electron collisions. The horizontal axis is the electron velocity (m/s × 10^5) and the vertical is Δv.

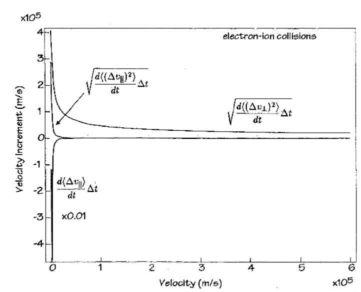

Figure 3. The same as Figure 2 but for electron-ion collisions.

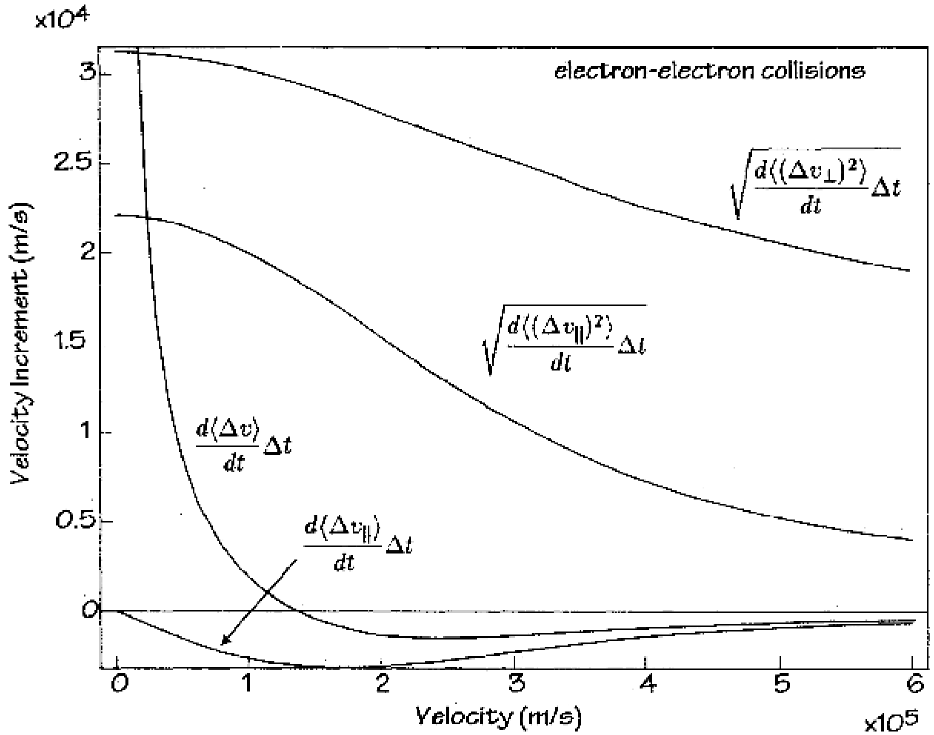

$$\frac{d\langle\Delta v_\parallel\rangle}{dt} = -A_D l_f^2 \left(1 + \frac{m_e}{m_f}\right) G(l_f v) \quad (13)$$

$$\frac{d\langle(\Delta v_\parallel)^2\rangle}{dt} = \frac{A_D}{v} G(l_f v) \quad (14)$$

$$\frac{d\langle(\Delta v_\perp)^2\rangle}{dt} = \frac{A_D}{v} \{\phi(l_f v) - G(l_f v)\} \quad (15)$$

where

$$A_D = \frac{n_f e^4 \ln \Lambda}{2\pi m_e^2 \epsilon_0^2}. \quad (16)$$

A_D differs from the definition of *Spitzer* [1962] only in that the units have been changed from cgs to MKS. Also $l_f^2 = m_f/2kT$; f designates the field particles, the ones being collided with, either e for electron or i for ion, while m_e refers to the test particle which is always an electron. We have assumed that all species have a charge number of 1. Finally,

$$G(x) = \frac{\phi(x) - x\phi'(x)}{2x^2} \quad (17)$$

where

$$\phi(x) = \frac{2}{\pi^{\frac{1}{2}}} \int_0^x e^{-y^2}\, dy \quad (18)$$

The update equations above constitute jointly the Langevin equation of a multivariate Markov process (non-linear and non-Gaussian) consisting of the components of $\mathbf{r}(t)$ and $\mathbf{v}(t)$. Estimates of ACF $\langle e^{j\mathbf{k}\cdot\Delta\mathbf{r}}\rangle$ were formed as the inverse Fourier transform of power spectra of synthesized time-series $e^{j\mathbf{k}\cdot\mathbf{r}(t)}$. In spectrum calculations standard FFT methods were employed, just like in radar data analysis. A *library* of Gordeyev integrals derived from simulated $\langle e^{j\mathbf{k}\cdot\Delta\mathbf{r}}\rangle$ is used ultimately for density spectrum calculations.

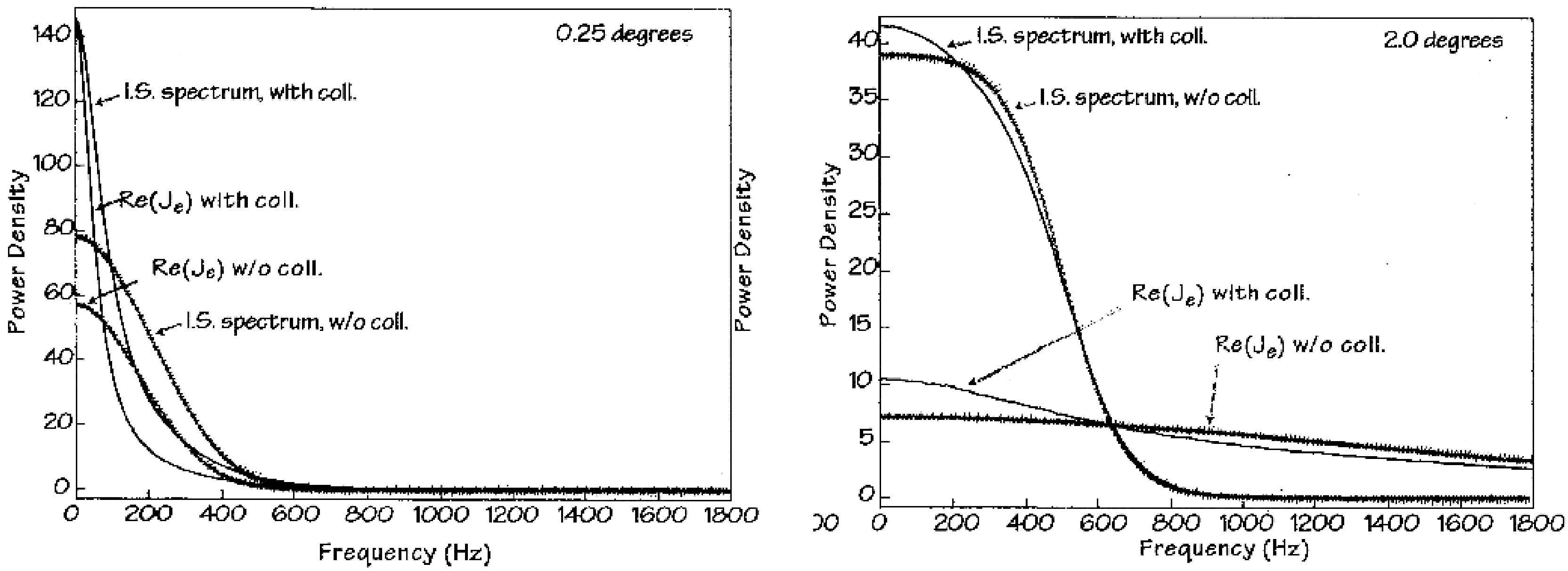

- Simulated *versus* collisionless spectra show considerable differences at small aspect angles α, enough to correct the T_e/T_i problem at $\alpha \approx 2^\circ$ measurements.
- *Woodman* [2004] re-examined the Brownian model and — agreeing with the main findings of *Sulzer and Gonzalez* — developed an empirical collision-frequency model $\nu_e = \nu_e(\alpha)$ that gives the best fit of Brownian spectra to *Sulzer and Gonzalez* [1999] simulation results.

- Woodman model $\nu_e = \nu_e(\alpha)$ effectively extrapolates the *Sulzer and Gonzalez* simulation results from $\alpha = 0.25^\circ$ to 0^o and is convenient to use in place of the *Sulzer and Gonzalez* Gordeyev library.

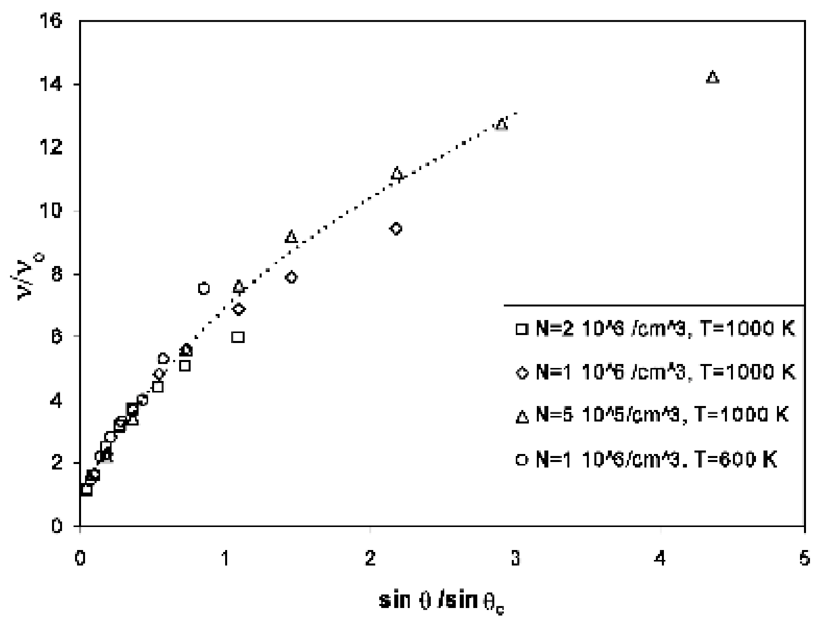

Fig. 6. Same as in Fig. 5 but both the collision frequency and the angle (actually sinθ) are normalized with respect to ν_0 and sin θ_c, respectively. The dotted line is a cubic regression fit representing Eq. (14). The points corresponding to 6° (right most in any sequence) are not included in the fit.

with $\sin\theta_c = \frac{\lambda}{\ell} = \frac{\lambda\nu_e}{C_e}$.

Highlights of Milla and Kudeki [2006] poster:

- Studies described in *Milla and Kudeki* [2006] aim to:
  - explore the goodness of Woodman's $\nu_e = \nu_e(\alpha)$ model in $\alpha \to 0$ limit and at radar wavelengths other than 3 m for which the model was developed,
  - improve the model if needed
- by using the same methodology as *Sulzer and Gonzalez* [1999], except for:
  - include finite gyro-radius effects by doing 3-D computations of particle orbits instead of 1-D (parallel $\mathbf{B}_o$) computations
  - extend the computations all the way to $\alpha = 0$.
- Initial results:
  - agree with *Sulzer and Gonzalez* [1999] results except for a minor offset (~10% near spectral peak as $\alpha \to 0.25^\circ$) the source of which was identified in Sulzer's code — a typo that replaces some $\sqrt{2}$ by $\sqrt{\pi/2}$.
  - Woodman's $\nu_e = \nu_e(\alpha)$ model inherits the offset just described but otherwise agrees with the simulated spectrum variations as $\alpha \to 0$.
  - Woodman's $\nu_e = \nu_e(\alpha)$ model needs "retuning" at other radar wavelengths (that is, other than at 50 MHz)

Last 1000 millidegrees of α:

$\mathrm{Re}\{J_e(\omega)\}$ at 50 MHz:

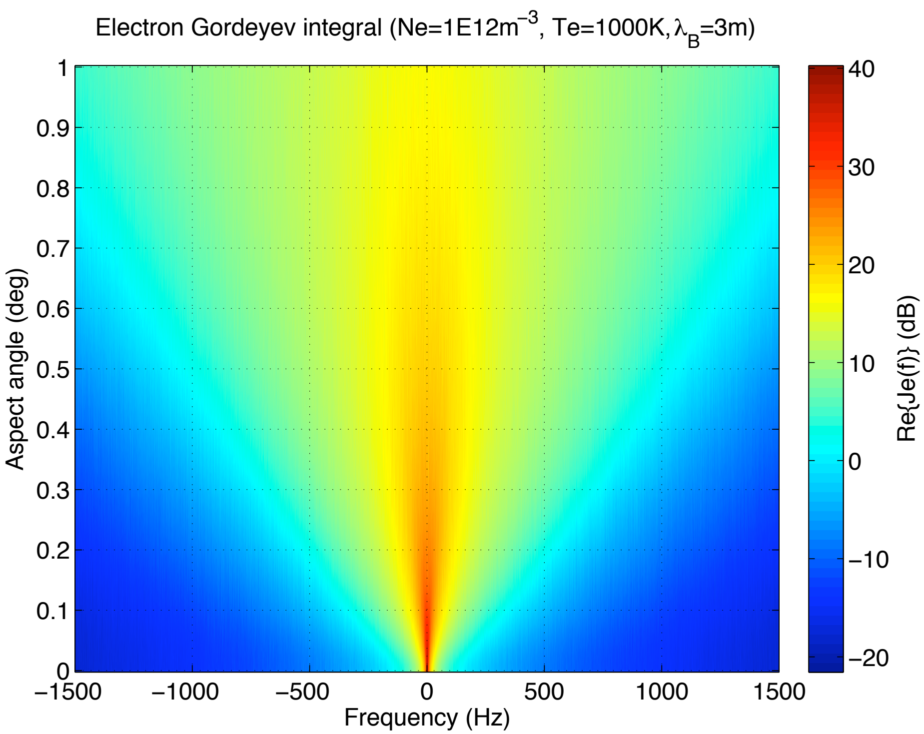

$\mathrm{Re}\{J_e(\omega)\}$ at 500 MHz:

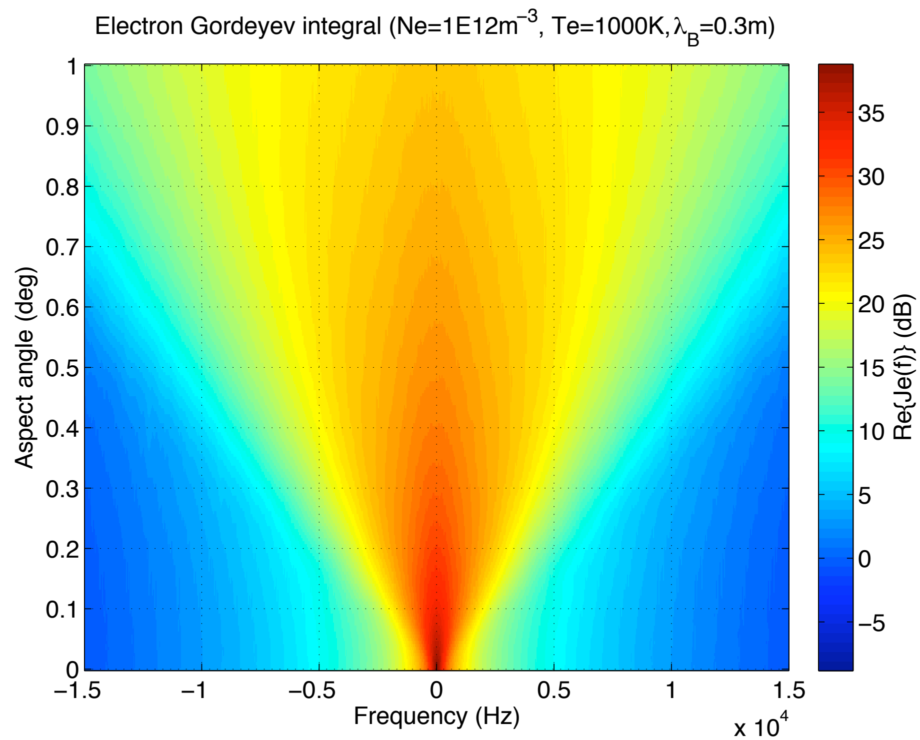

Note how $\langle|n_{te}(\mathbf{k},\omega)|^2\rangle \propto \mathrm{Re}\{J_e(\omega)\}$ narrows down more rapidly at 50 MHz than at 500 MHz as approaches $\alpha = 0$.

A "testable" prediction using a pair of ISR's — VHF and UHF — near the magnetic equator: ALTAIR or, alternatively, JRO/AMISR combo.

Last 500 millidegrees of α:

$\mathrm{Re}\{J_e(\omega)\}$ at 50 MHz:

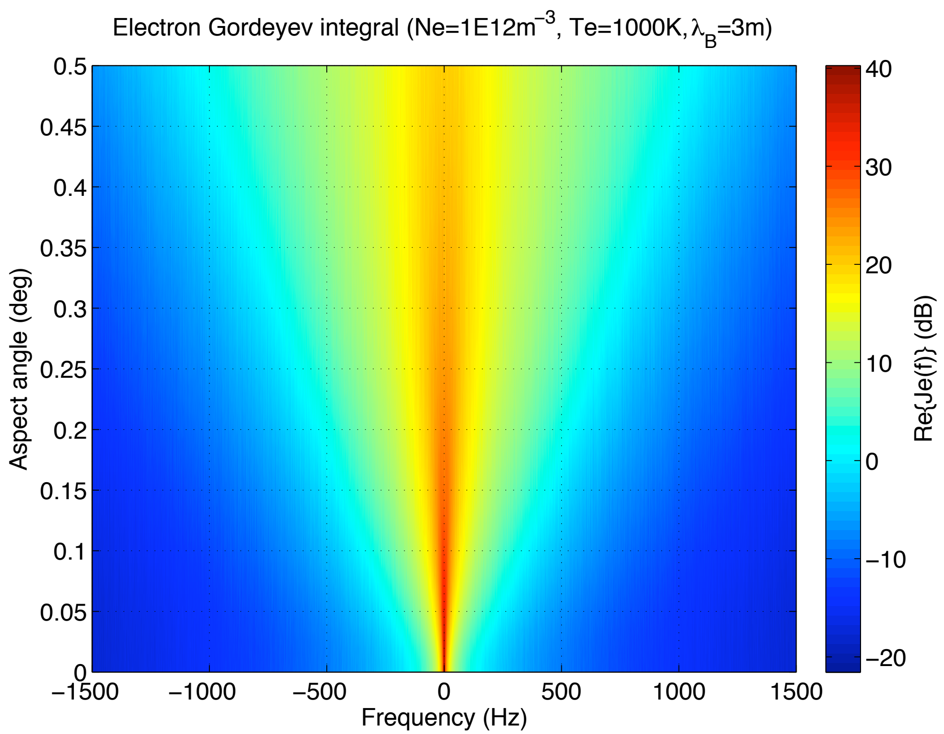

$\mathrm{Re}\{J_e(\omega)\}$ at 500 MHz:

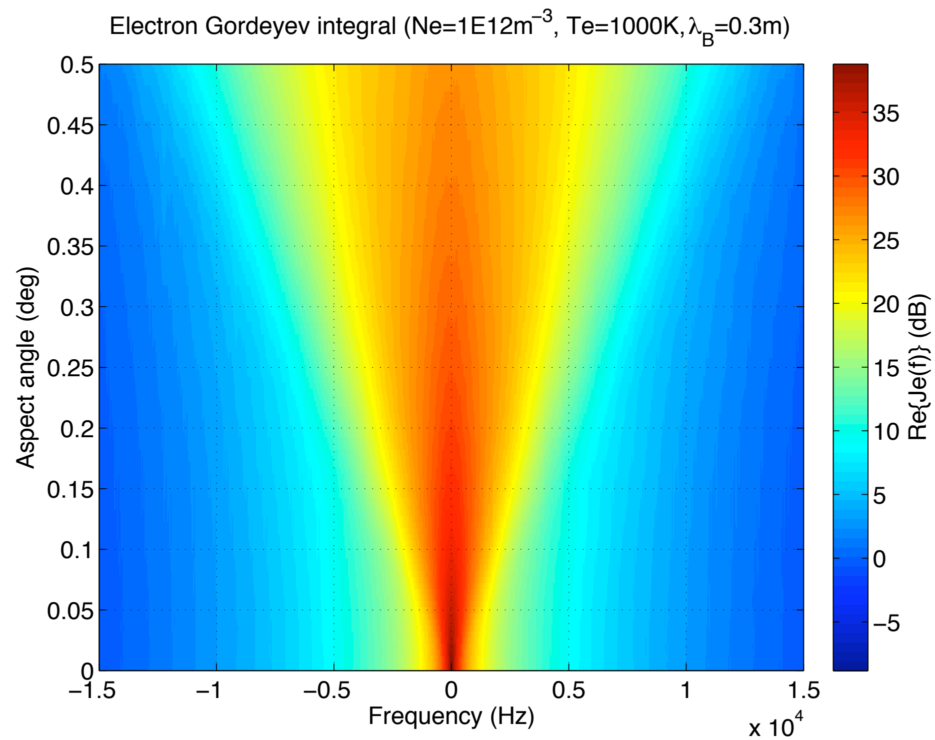

Note how $\langle|n_{te}(\mathbf{k},\omega)|^2\rangle \propto \mathrm{Re}\{J_e(\omega)\}$ narrows down more rapidly at 50 MHz than at 500 MHz as approaches $\alpha = 0$.

A "testable" prediction using a pair of ISR's — VHF and UHF — near the magnetic equator: ALTAIR or, alternatively, JRO/AMISR combo.

More detailed comparisons show that:

1. Brownian motion based *ion*-Gordeyev integrals match ion Monte Carlo results very well using for ν_i the effective Coulomb collision frequency (due to Spitzer) for ions given earlier. This finding is consistent with the success of *Woodman* [1967] theory in showing the absence of ion gyro-resonance effects.
2. Monte Carlo results for electron displacements Δp transverse to $\mathbf{B}_o$ exhibit a Gaussian Δp with a variance $\langle \Delta p^2 \rangle$ matching well the Brownian motion model using $\frac{5}{3}\nu_e$ for ν, where ν_e is the Spitzer collision frequency for electrons. The factor $5/3$ is independent of N_e and T_e, and is likely to be due to electron-electron collisions not included in Spitzer's ν_e.
3. Monte Carlo results show that Δr for electrons is a *non-Gaussian* random variable for $\tau \sim \nu_e^{-1}$ and Gordeyev integrals obtained from Brownian motion versus Monte Carlo calculations do not match except in $\alpha \longrightarrow 0$ limit.
4. Modified Brownian model of *Woodman* [2004] shows a reasonable agreement with the simulations at 50 MHz (3 m radar) except for a minor offset, but it requires adjustments at higher probing frequencies such as 500 MHz (30 cm radar).
5. Electron-collision effects are less pronounced for a 30 cm radar than for 3 m radar (as expected), but still the effects cannot be neglected at small α.

At very very small aspect angles, 1 and 5 *milli-degrees* ($T_{e,i} = 1000$ K, O^+):

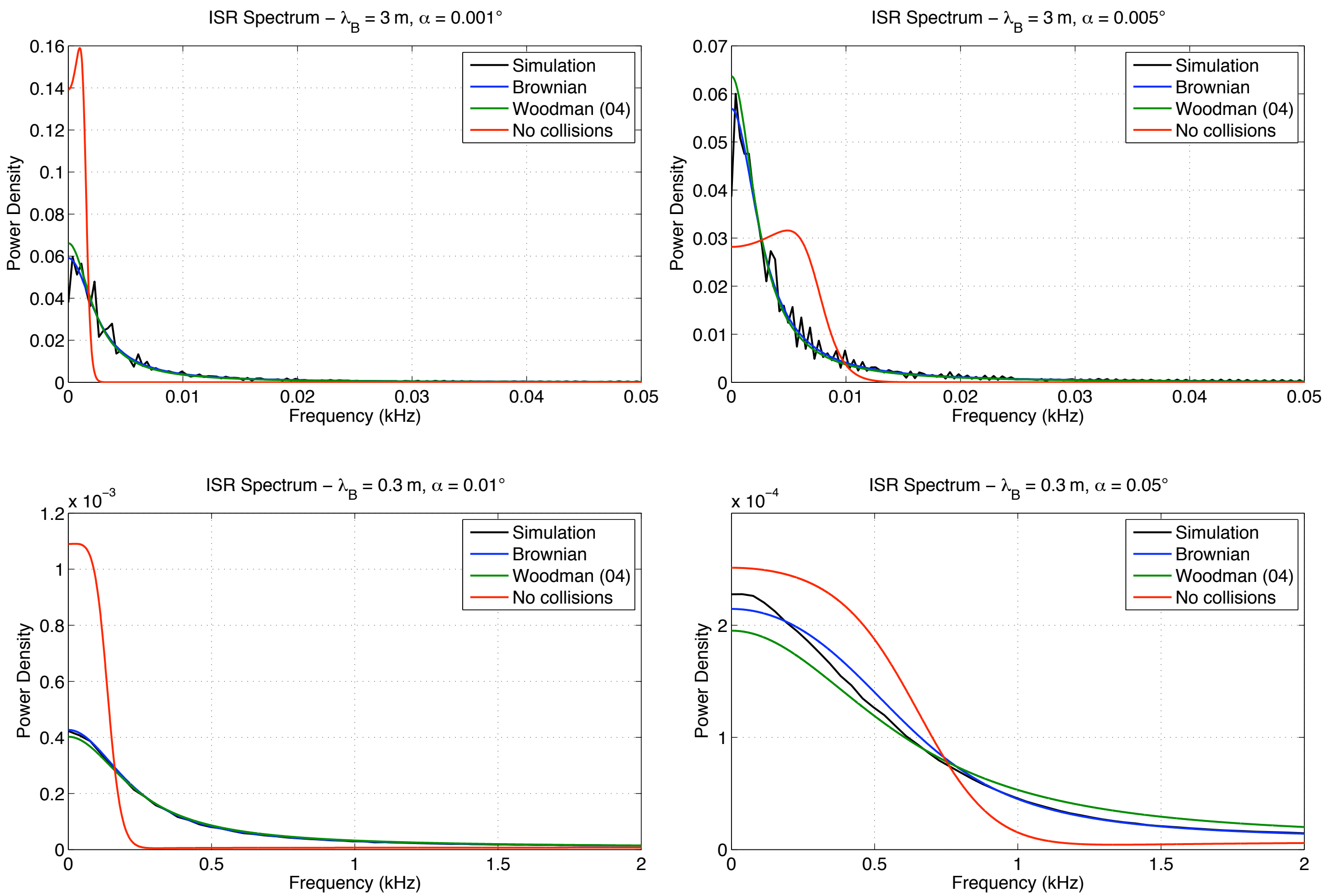

At perp. to $\mathbf{B}$ (collisionless is a δ here) and at 0.5° off-perp.:

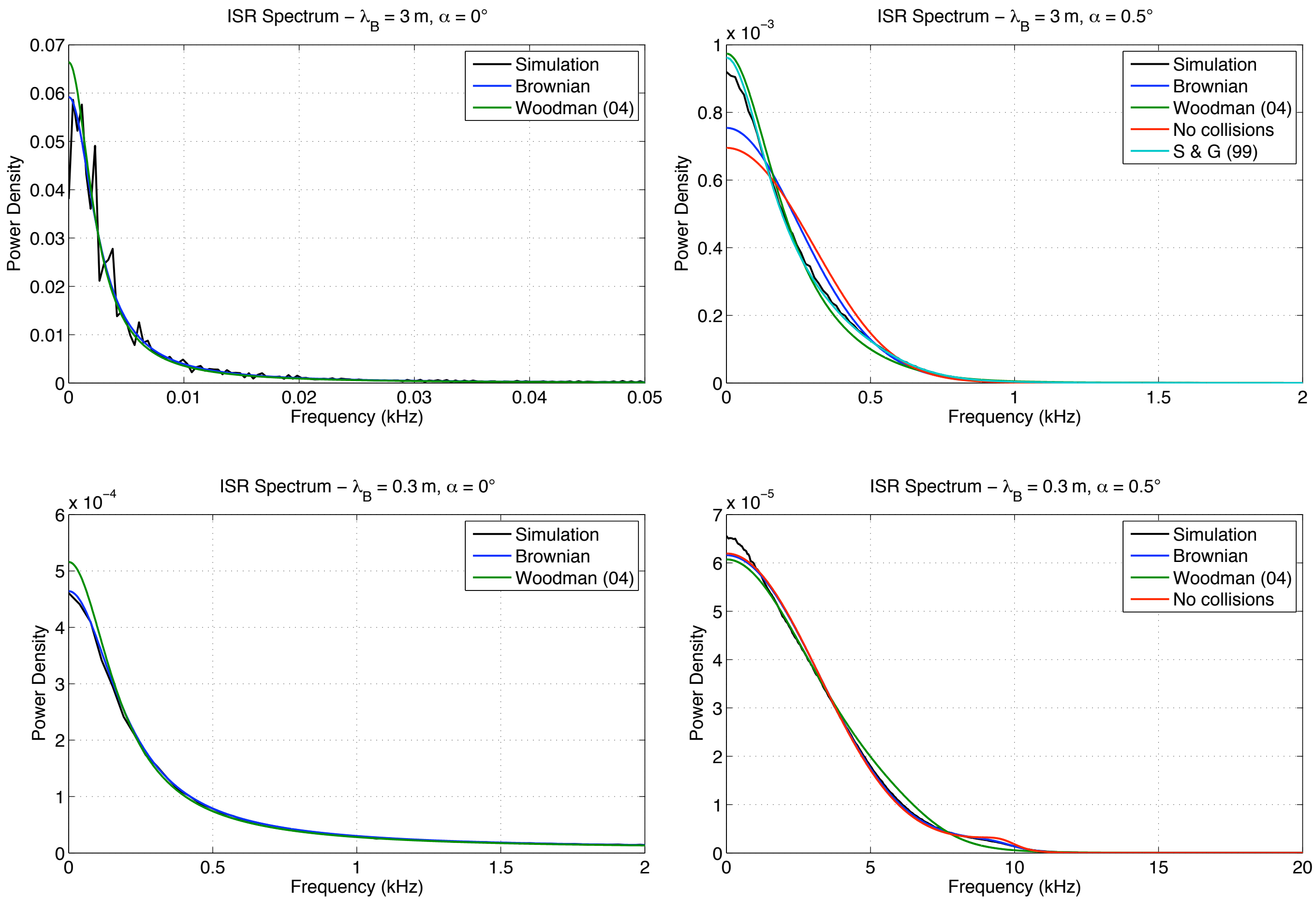

Conclusions

- *Sulzer and Gonzalez* [1999] simulations of electron-Coulomb collisions and their impacts on ISR spectra at small aspect angles were — *for all practical purposes* — **confirmed** by our simulations, which were conducted with independent software and algorithms using a 3-D setting (instead of 1-D).
- The extension of the simulations to $\alpha = 0$ has shown that *Woodman* [2004] semi-empirical model works well at 50 MHz except for the need for a minor correction of a minor error inherited from *Sulzer and Gonzalez* [1999] simulations.
- The extension of simulations from 50 MHz to 500 MHz have provided the information to generalize the semi-empirical model for use over a range of practical ISR frequencies.
- We have now a working small-α spectral theory to subject it to further *experimental tests* and attempt inversions of measured ISR spectra at small-α for densities and temperatures based on the new model.
- We are optimistic that T_e *and* T_i can be estimated by using both *spectral* and *cross-spectral* data — north-south baseline cross-spectra are sensitive to T_e/T_i dependent "aspect sensitivity" of incoherent scattered signal.

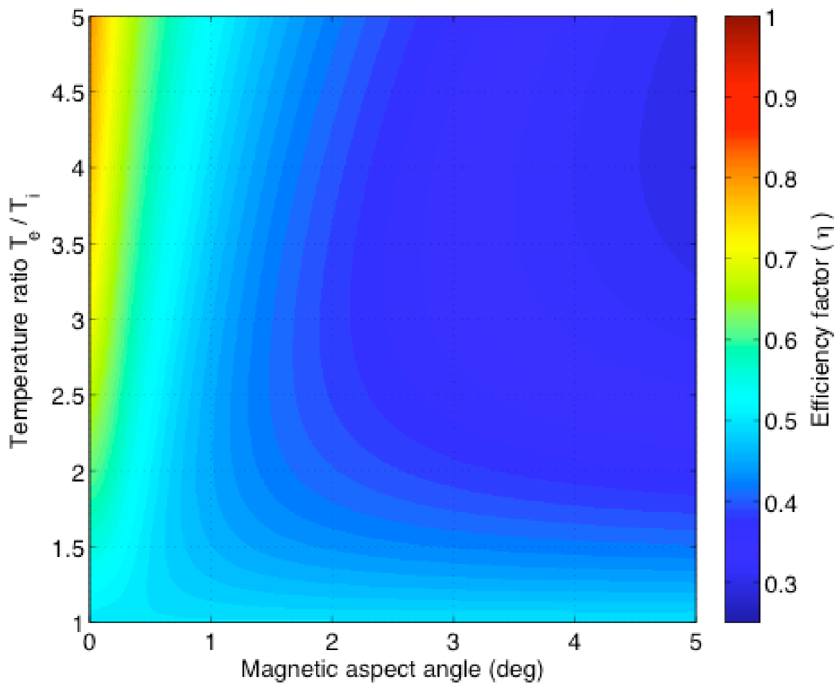

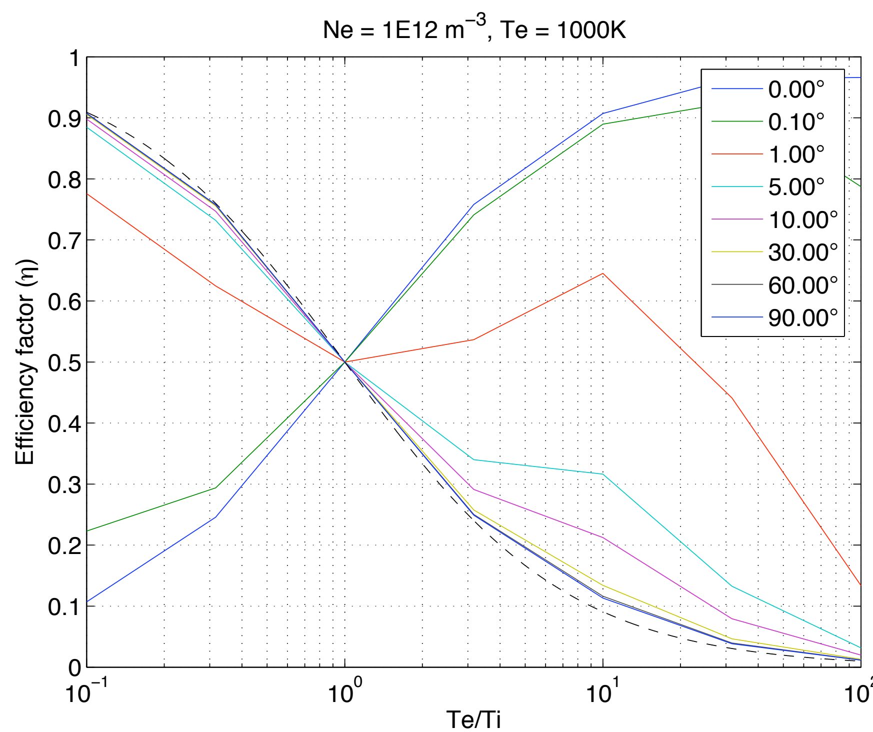

References (and with thanks to...)

Aponte, Sulzer, and Gonzalez [2001]

Bowles [1958]

Chandrasekhar [1942]

Callen and Greene [1952]

Daugherty and Farley [1963]

Farley, Dougherty, and Barron [1961]

Farley [1964]

Fejer [1961]

Feng, Kudeki, Woodman, Chau, and Milla [2004]

Gillespie [1995]

Hagfors and Brockelman [1971]

Hysell and Kudeki [2004]

Kudeki, Bhattacharyya, and Woodman [1999]

Kudeki and Bhattacharyya [1999]

Mathews [1978]

Milla and Kudeki [2006, Cedar Poster]

Pingree [1990]

Rosenbluth, MacDonald, and Judd [1957]

Spitzer [1958]

Sulzer and Gonzalez [1999]

Woodman [1967]

Woodman [2004]